Chemical Science

ROYAL SOCIETY OF CHEMISTRY

EDGE ARTICLE

View Article Online
View Journal | View Issue



Cite this: *Chem. Sci.*, 2021, **12**, 10347

All publication charges for this article have been paid for by the Royal Society of Chemistry

Received 20th February 2021
Accepted 28th June 2021

DOI: 10.1039/d1sc01013a

rsc.li/chemical-science

# Easily accessible non-aromatic heterocycles with handles: 4-bromo-2,3-dihydrofurans from 1,2-dibromohomoallylic alcohols†

Jason An, Jose Intano, Jr., Alissa Richard, Taehyun Kim, José A. Gascón * and Amy R. Howell *

The first general preparation of 4-bromo-2,3-dihydrofurans is reported. These non-aromatic heterocycles containing a useful coupling handle are accessed *via* Cu-catalyzed intramolecular cyclization of 1,2-dibromohomoallylic alcohols, which are themselves available in just two steps from aromatic and aliphatic aldehydes and ketones. Molecular dynamics simulations using the simple substrates and key geometric parameters provide a rationale for the selectivities observed. The synthetic utility of the 4-bromodihydrofurans is also demonstrated.

## Introduction

Non-aromatic heterocycles are ubiquitous in nature and widely targeted in synthetic methodology development.[1,2] While the ability to diversify aromatic heterocycles has exploded with the development of a range of cross coupling methodologies exploiting aromatic heterocycles with reactive handles,[3–8] ready access to non-aromatic heterocycles with such handles is lacking. We have been interested in functionalized non-aromatic heterocycles that can be used as templates for diversification. For example, we have shown that α-methylene-β-lactones **1** undergo cross-metathesis or rhodium catalysed conjugate addition, making them scaffolds with broad utility (Fig. 1A).[9–11] It occurred to us that the cyclization of 1,2-dibromohomoallylic alcohols **2** had the potential to provide either 4-bromo-2,3-dihydrofurans **3** or 2-bromomethyleneoxetanes **4** (Fig. 1B). While either outcome would satisfy our interest in diversifiable scaffolds, the utility of this method would be best served by selectivity in the cyclization.

Metal-mediated intramolecular reactions using vinylhalides have been used to prepare oxetanes.[12] Intramolecular preparations of dihydrofurans have largely been limited to the cyclization of aryl halides to give dihydrobenzofurans.[13,14] These approaches, however, do not inherently provide a handle for diversification subsequent to cyclization. Geminal dibromides have been used extensively in the preparation of benzofurans.[15] Although the cyclized products have a handle, the products are almost exclusively aromatic heterocycles; our interest is in non-aromatic heterocycles. To our knowledge, there is no literature precedent using vicinal dihalides (as in **2**). We anticipated that the presence of two halogens on the double bond would impact selectivity and yields (due to more competing potential outcomes). Herein we report the results of our exploration of the cyclization of 1,2-dibromohomoallylic alcohols and computational studies to understand the selectivities observed.

## Results and discussion

The initially investigated dibromoalkenol **2a** was prepared in two steps, propargylation and dibromination (*vide infra*), from benzaldehyde. It was treated with CuI under typical conditions[14] for Ullmann-type cyclizations (Table 1, entry 1) and gave mainly one product in 60% isolated yield. Proton/carbon NMR experiments confirmed that it was dihydrofuran **3a**. This result was important because there are no literature reports of a general preparation of 4-bromo-2,3-dihydrofurans. Such systems would

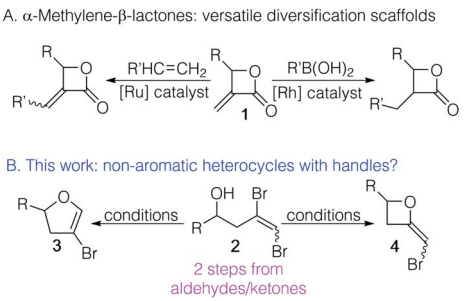


Fig. 1 Non-aromatic heterocycles with handles: (A) α-methylene-β-lactones **1** can be used to access diverse β-lactone motifs; (B) 1,2-dibromohomoallyic alcohols could provide non-aromatic heterocycles **3** and/or **4** with a handle for functionalization.

*Department of Chemistry, University of Connecticut, Storrs, CT 06269, USA. E-mail: amy.howell@uconn.edu; jose.gascon@uconn.edu*

† Electronic supplementary information (ESI) available: Experimental details, spectroscopic data for all new compounds, computational methods (PDF). See DOI: 10.1039/d1sc01013a

Table 1 Optimization of Cu(I)-catalyzed cyclization of **2a**

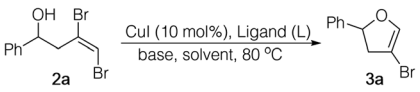


| Entry | L[a], base (equiv.) | Solvent | Conv[b] (yield)[c] |
|---|---|---|---|
| 1[d] | **A**, $Cs_2CO_3$ (2) | $CH_3CN$ | 86 (60) |
| 2[e] | **A**, $Cs_2CO_3$ (2) | $CH_3CN$ | 66 |
| 3[f] | **A**, $Cs_2CO_3$ (2) | $CH_3CN$ | 100 (76) |
| 4[f,g] | **A**, $Cs_2CO_3$ (2) | $CH_3CN$ | 49 |
| 5[f] | **A**, $Cs_2CO_3$ (1.2) | $CH_3CN$ | 100 (80) |
| 6[f] | **A**, $Cs_2CO_3$ (1.2) | $MeNO_2$ | 0 |
| 7[f] | **A**, $Cs_2CO_3$ (1.2) | DMF | 29 |
| 8[f] | **A**, $Cs_2CO_3$ (1.2) | THF | 100 (69) |
| 9[f] | **B**, $Cs_2CO_3$ (1.2) | $CH_3CN$ | 75 |
| 10[f] | **C**, $Cs_2CO_3$ (1.2) | $CH_3CN$ | 12 |
| 11[f] | **D**, $Cs_2CO_3$ (1.2) | $CH_3CN$ | 61 |
| 12[f] | **A**, NaOtBu (1.2) | $CH_3CN$ | 58 |
| 13[f] | **A**, TMSOK (1.2) | $CH_3CN$ | 22 |
| 14[f] | No L, $Cs_2CO_3$ (1.2) | $CH_3CN$ | 12 |
| 15[f] | No Cu/L, $Cs_2CO_3$ (1.2) | $CH_3CN$ | 0 |

[a] Ligands (L): **A** = 1,10-phenanthroline; **B** = L-proline; **C** = BINOL; **D** = BINAP. [b] Conversion was estimated from $^1$H NMR and is based on relative amounts of starting material and dihydrofuran. [c] Isolated yield of **3a**. [d] Concentration of **2a** = 0.1 M; reaction time = 8 h. [e] Concentration of **2a** = 0.05 M; reaction time = 8 h. [f] Concentration of **2a** = 0.05 M; reaction time = 16 h for entries 3–15. [g] CuBr (10 mol%) rather than CuI.

Table 2 Dibromination of homopropargyl alcohols **5** and subsequent Ullmann-type cyclization of **2**

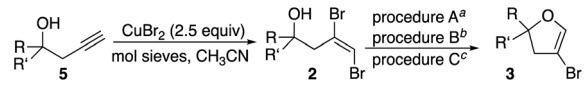


| Compound | R | R′ | Yield of **2** | Yield of **3**[d] | Yield of **3**[c] |
|---|---|---|---|---|---|
| **a** | Ph | H | 89 | 78[a] | 88 |
| **b** | *p*-Toly | H | 78 | 86[a] | |
| **c** | 4-*t*-BuPh | H | 89 | 74[a] | 87 |
| **d** | 4-FPh | H | 86 | 67[a] | 62 |
| **e** | 4-$CF_3$Ph | H | 82 | 69[a] | |
| **f** | $CH_3(CH_2)_8CH_2$ | H | 85 | 63[b] | 70 |
| **g** | Cyclohexyl | H | 80 | 65[b] | 57 |
| **h** | $PhCH_2CH_2$ | H | 84 | 72[b] | 74 |
| **i** | $PhCH_2OCH_2$ | H | 25 | 82[b] | |
| **j** | Ph | $CH_3$ | 85 | 79[a] | |
| **k** | $CH_3(CH_2)_7CH_2$ | $CH_3$ | 86 | 74[b] | |
| **l** | 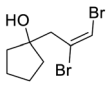 | | 85 | 68[b] | 52 |
| **m** | 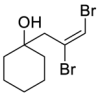 | | 69 | 67[b] | |
| **n** | 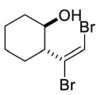 | | 61 | 80[b] | 88 |

[a] Procedure A: CuI (10 mol%), 1,10-phenanthroline (20 mol%), $Cs_2CO_3$ (1.2 equiv.), $CH_3CN$, 80 °C, 16 h, concentration = 0.05 M. [b] Procedure B: CuI (10 mol%), 1,10-phenanthroline (20 mol%), $Cs_2CO_3$ (1.2 equiv.), 1,4-dioxane, 115 °C, 16 h, concentration = 0.05 M. [c] Procedure C: CuBr (10 mol%), 1,10-phenanthroline (20 mol%), $Cs_2CO_3$ (1.2 equiv.), 1,4-dioxane, 115 °C, 16 h, concentration = 0.05 M. [d] **2a–n** cyclized with procedure A or B contained 1–11% of the corresponding inseparable iodide **6** (see discussion and ESI). Yields are based on just bromide **3**.

be valuable for coupling reactions, leading to functionalized dihydrofurans. Our first goals were to optimize the transformation, then explore its scope. If the 5-*endo*-cyclization was general, a related goal was to understand the preference for the formation of bromodihydrofurans **3** over bromomethyleneoxetanes **4**.

Although the initial isolated yield was reasonable (Table 1, entry 1), several byproducts were observed in the crude $^1$H NMR spectrum. We anticipated that variations described in the literature for intramolecular Ullmann-type coupling would lead to improved yields.[14] Decreasing the concentration (entry 2) gave a cleaner reaction, but lower conversion. Doubling the reaction time resulted in complete conversion (entry 3). CuBr promoted clean formation of **3a**, but the conversion was significantly lower over the same time period (entry 4). Decreasing the base loading did not substantially change the outcome for **2a** (entry 5), but it was found to be critical for ketone-derived substrates (*e.g.* **2j**, Table 2), where the higher base loading gave considerable return of initial ketone. Changing the solvent (entries 6–8), the ligand (entries 9–11) and the base (entries 12–13) did not improve the outcome. While a little product was formed without the ligand (entry 14), no conversion occurred without CuI (entry 15). Overall, the best yield for the preparation of **2a** resulted from the conditions shown in entry 5 (Table 1).

In order to examine the scope of the cyclization, additional dibromoalkenes **2b–n** were prepared. This was achieved in two straightforward and efficient steps. Homopropargyl alcohols **5** were readily prepared by zinc-mediated propargylation of the corresponding aldehydes and ketones.[16] These were efficiently converted to *E*-dibromoalkenes **2** by treatment with $CuBr_2$ in the presence of activated molecular sieves.[17] Of note, these latter conditions were incompatible with highly electron rich aromatic compounds (*e.g.*, *p*-MeOPh, thiophene).

The dibromoalkenes **2b–e**, derived from aromatic aldehydes, were converted in very good yields to the corresponding 4-bromodihydrofurans **3b–e** (Table 2) under the conditions optimized for **2a** (procedure A). In contrast, for dibromoalkene **2f**, which came from undecanal, procedure A provided only 37% yield of **3f**. Although heating in acetonitrile at 80 °C for a longer period improved the conversion, a better outcome was realized by switching to 1,4-dioxane (oil bath temperature 115 °C). Using dioxane, 4-bromodihydrofurans **3f–i** were prepared in very good yields (procedure B, Table 2). With the exception of dibromide **2j**, which cyclized efficiently under the milder conditions of procedure A (Table 2), dibromoalkenes (**2k–m**) derived from ketones also cyclized with improved yields when refluxing

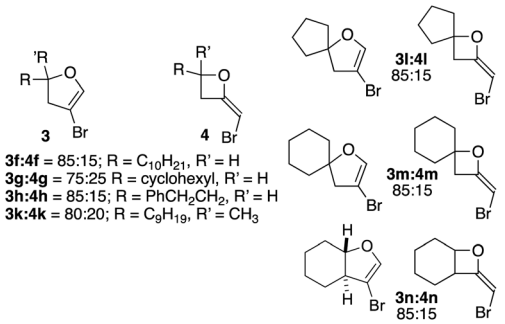


Fig. 2 Ratio of 4-bromodihydrofurans **3** to 2-bromomethyleneoxetanes **4** in cyclizations of homopropargylic alcohols derived from aliphatic aldehydes/ketones.

dioxane was used. Ketone derived **2l** and **2m** provided interesting spirocyclic bromodihydrofurans **3l** and **3m** while alcohol **3n**, prepared in two steps from cyclohexane oxide, gave fused bromodihyrofuran **3n** (see Fig. 2). Overall, a wide range of easily accessible *trans*-vinyldibromides was converted to 4-bromodihydrofurans in very good to excellent yields.

Analysis of the $^1$H NMRs of spirocyclic furans **3l** and **3m** led to an interesting observation. For both compounds there was a small doublet just upfield from the doublet for the allylic $CH_2$. Assuming this might be an allylic signal of a related compound, the integration for this unknown product represented ~5–10% yield in comparison to **3l** or **3m**. Distinct or shadow peaks in the $^{13}$C NMR spectra confirmed the presence of a related product. Attempts to separate this impurity were unsuccessful. Examination of the $^1$H NMR spectra of other dihydrofurans **3** showed at least hints of upfield allylic proton peaks in all of them. A combination of the similarity of the NMR spectra and a faint pink tinge in NMR solutions that had set for some time led us to suspect that 4-bromo-2,3-dihydrofurans **3l** and **3m** contained 4-iododihydrofurans **6l** and **6m**. This was confirmed by GC/MS, which showed that all of the dihydrofurans contained some of the corresponding iodides (from 1–11% – see ESI† for details). The yields of **3** given in Table 2 are for just the bromides. It is noteworthy that the attractiveness of the bromide lies in its utility as a handle for subsequent coupling transformations, and the iodides would be as or more reactive.

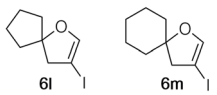


The fact that every 4-bromodihydrofuran prepared contained at least some of the corresponding iodide **6** led us to reconsider CuBr as a catalyst, although we had abandoned it because of the slower conversion to product (Table 1, entry 4). When dibromide **2a** was heated in dioxane containing CuBr (10 mol%), 1,10-phenanthroline (20 mol%) and $Cs_2CO_3$ (1.2 equiv.) (procedure C, Table 2, last column), 4-bromodihydrofuran **3a** was isolated in 88% yield. Gratifyingly, dibromides derived from both aliphatic and aromatic aldehyde precursors could be cyclized with yields similar to those realized with the CuI (Table 2, column 5).

We decided to see if the cyclization strategy could be extended to an internal dibromoalkene and one with substituents on the allylic carbon; so compounds **7** and **10** were prepared (see ESI†). For internal alkene **7**, both procedures A and B (Table 2) resulted only in recovery of the starting material. However, when alkene **7** was treated with CuI (20 mol%) in the presence of $Cs_2CO_3$ (2 equiv.) without ligand in dioxane (oil bath temperature 115 °C), $^1$H NMR showed starting material (~50%) and two products, formed in an approximately 1 : 1 ratio. Through NMR experiments we deduced that one of the products was 2-bromomethyleneoxetane **8**; the other was the expected bromodihydrofuran **9**. In a related outcome, dibromoalkene **10** gave oxetane **11** and dihydrofuran **12**, also in an approximately 1 : 1 ratio. Interestingly, the combined yield of **11**/**12** was only 24% with some starting material remaining under procedure A (Table 1). Moreover, the crude $^1$H NMR was unusually messy. In contrast, with procedure C the combined yield of the two products (**11** : **12** ratio of 42 : 58) was 73%, and the crude $^1$H NMR showed only the two products. The outcomes with **7** and **10** were significant in that they showed that the preferential, and seemingly exclusive, formation of 5-*endo* products was not straightforward.

The fact that $^1$H NMR chemical shifts for bromomethyleneoxetanes **8** and **11** were generally downfield from those of dihydrofurans **9** and **12** led us to recall earlier observations. Crude $^1$H NMRs for the cyclizations of aliphatic systems **2f–h** and **2k–n** had shown varying amounts of a proton signal downfield from that of C2 of the dihydrofurans (see Scheme 1 for numbering). These byproducts were not seen in any fractions from the columns. It occurred to us that this signal could be associated with 2-bromomethyleneoxetanes **4**. Our own experience had shown that 2-methyleneoxetanes are generally unstable to normal flash silica gel.[18] Running the reactions of **2f–h** and **2k–n** again, followed by purification on deactivated silica, provided mixtures that contained dihydrofurans **3f–h** and **3k–n** and the products associated with the signal appearing downfield from the C2 signal of bromodihydrofurans **3**. In the case of the cyclization of **2h**, running a second column on deactivated silica provided a clean sample of **4h** (see Fig. 2 and ESI†). The isolation of **4h** and **8** and **11** and comparison of their NMR spectra with those of the mixtures isolated from deactivated silica confirmed that varying amounts of brominated methyleneoxetanes **4f–h** and **4k–n** were being formed as minor products, along with dihydrofurans **3f–h** and **3k–n**. It should be stressed that the yields in Table 2 for the formation of **3**

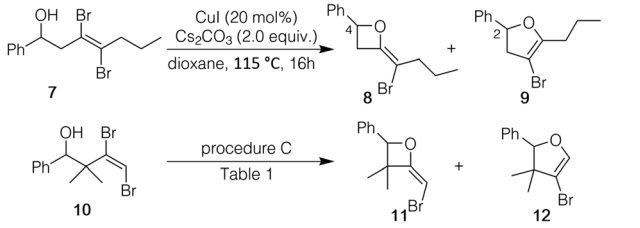


Scheme 1 Cyclization of internal dibromoalkene **7** and of a dibromoalkene (**10**) with allylic substitution.

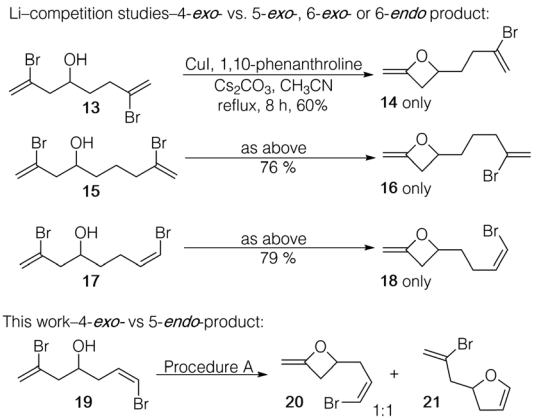


Scheme 2 Competition studies.

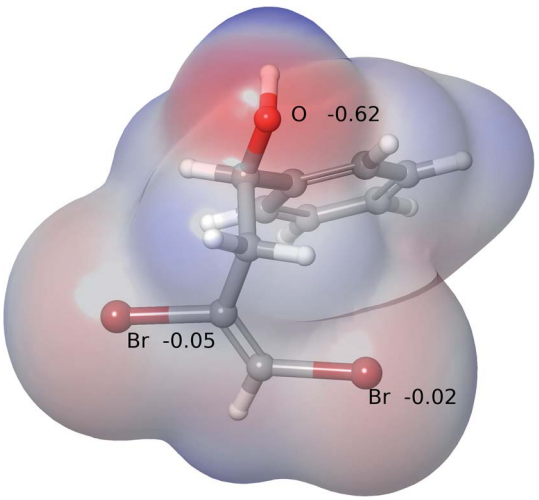


Fig. 3 Electrostatic potential map of **2a** showing ESP charges on O and Br atoms.

accurately reflect those for the dihydrofurans, as bromomethyleneoxetanes **4f–h** and **4k–n** were destroyed on untreated silica. No bromomethyleneoxetanes were seen in the cyclizations of benzylic alcohols **2a–e** and **2j** or **2i**. The ratios of dihydrofuran to oxetane in the cyclizations of **2f–h** and **2k–n** (based on crude $^1$H NMR) are shown in Fig. 2. Taken together, the results with **7** and **10** and with the aliphatic systems **2f–h** and **2k–n** made us wonder if there is an inherent difference in 4-*exo vs.* 5-*endo*-selectivity with these CuI/CuBr promoted reactions.

Fang and Li had conducted selectivity studies in their report on the preparation of 2-methyleneoxetanes by Cu-mediated cyclization of vinyl bromides.[12] In their study, alcohols were prepared that had two bromoalkene moieties that allowed for competing product formation *via* 4-*exo*- or 5-*exo*-modes (see **13**, Scheme 2) or 4-*exo*- or 6-*exo*-modes (see **15**). Only the 4-*exo*-products **14** and **16** were isolated. Dienol **15**, which allowed for 4-*exo*- or 6-*endo*-product formation, also gave exclusively 4-*exo*-product (**18**). However, a 4-*exo*- *vs.* 5-*endo*-competition experiment was not reported. We prepared **19** (see ESI†), and with procedure A (Table 2), complete consumption of the starting material was observed with conversion to both 4-*exo*-**18** and 5-*endo*-**19** (in a 1 : 1 ratio based on crude $^1$H NMR). Thus, there is no inherent preference for the formation of 5-*endo*- over a 4-*exo*-product in a direct competition. Why, then, are we observing either exclusive or major formation of 5-*endo* products with 1,2-dibromoalkenes **2** (but not with **7** and **10**)?

It was tempting to view the preference for the formation of 5-*endo*-product as being a result of an electronic effect associated with vicinal 1,2-dibromoalkenes in comparison to the monobromo alkenes shown in Scheme 2. We investigated whether there could be any difference in the electron distribution around the proximal Br ($Br_P$) atom (proximal to O) and the distal Br ($Br_D$) atom (distal to O) (see Fig. 4 for labeling) that could affect selectivity. Fig. 3 shows the electrostatic maps of **2a** at its global energy minimum conformation, derived *via* a combination of force field conformational search and Density Functional Theory (DFT). The electrostatic potential charges (ESP) on the Br atoms are a very small fraction of the unit electron charge. They are an order of magnitude smaller than the charge on the oxygen atom and very similar to each other. Moreover, at finite temperature, we expect the two Br atoms to be electrostatically indistinguishable, ruling out any electronic origin affecting selectivity.

Considering Li's work and ours, it has been shown experimentally that Cu, presumably "guided" by its interaction with the alcohol oxygen, promotes the formation of 4-*exo* and/or 5-*endo* products. In the 4-*exo* outcome, the Cu complex undergoes oxidative addition of the proximal C–Br (see Fig. 4), while for the 5-*endo* product oxidative addition occurs with the distal C–Br. The question is: what controls selectivity? From mechanistic studies on related systems, we assume that Cu (ligated with phenanthroline in most of the cases we consider) first coordinates to oxygen.[19,20] Once this occurs, we hypothesize that oxidative addition would, in general, occur with the Br atom (taking into account a dynamical average) that is at an optimal distance to the oxygen atom. If that distance is too large the reaction will not occur. If such distance is too short, this will hinder the activation by Cu. To test this hypothesis and to address the impact of conformation and distance, we selected five representative compounds (**13**, **19**, **2a**, **7**, **2k**) that produce 4- and 5-member rings to various extents. Since these molecules exhibit several rotatable bonds, modeling conformational flexibility *via* molecular dynamics (MD) is of key importance. Such MD simulations should be at least a few orders of magnitude longer than the slowest vibrational modes, which are typically of the order of 1 ps. Thus, we performed a 10 ns MD simulation at 80 °C for all of these compounds, explicitly solvated by acetonitrile. Since for such time scales a quantum mechanical-based MD would be prohibited, we carried out MD simulations using the OPLS3e force field. This recently developed force field[21] represents the largest concerted parameterization effort aimed at organic molecules. In particular, it provides extensive parameterization of valence and torsional terms. MD simulations were carried out with Desmond, within the Schrodinger 2019-4 suite.[22] It is also important to note that we made no attempt to model the mechanism of Cu-phenanthroline

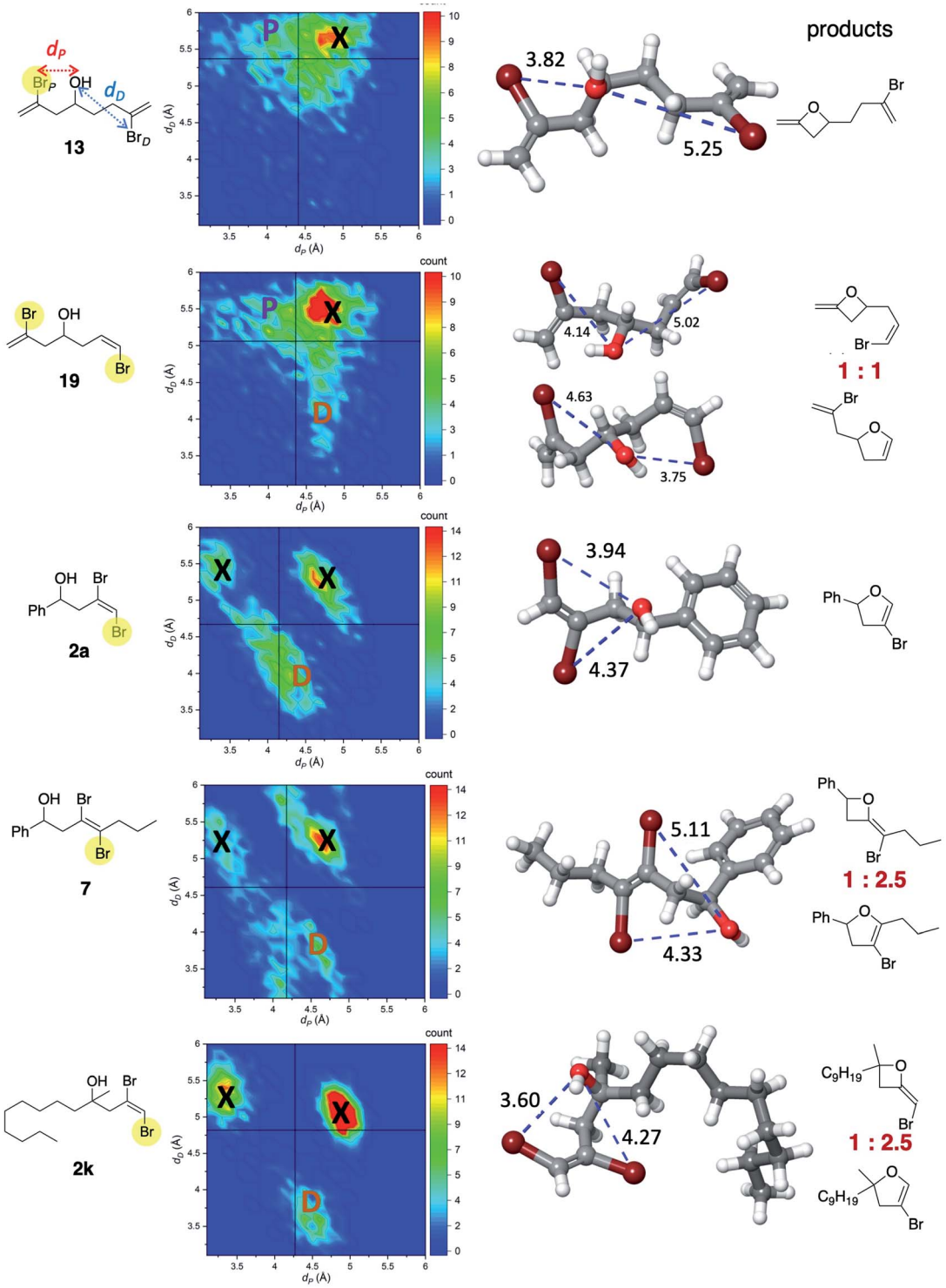


Fig. 4 Representative compounds (**13**, **19**, **2a**, **7**, **2k**) for which 4-*exo* and 5-*endo* products were experimentally observed. The second column presents a correlation map between $d_P$ and $d_D$ (annotated on compound **13**). The vertical and horizonal black lines correspond to the average value of these two distances. The third column shows typical snapshots of high-density regions in the correlation map, marked up with P (proximal) or D (distal). That is, these snapshots reflect the most abundant configuration that leads to either the oxidative addition of $Br_P$ or $Br_D$, and the subsequent formation of either 4-*exo* or 5-*endo*, respectively. The ratio *x* : *y* (in red) corresponds to the 4-*exo* : 5-*endo* ratio at 80 °C. Areas marked with X correspond to non-reactive configurations.

binding and oxidative addition. Instead, we simply probed whether there could be intrinsic conformations that may alone account for the observed selectivity.

Two key geometric parameters were monitored throughout the MD simulation: $d_P$ and $d_D$, as shown in the first structure in Fig. 4. Although there are other internal coordinates that may

correlate with oxidative addition selectivity, we found that these two alone presented a simple, qualitative correlation with the outcome of the reactions. The vertical and horizontal lines in the correlation maps correspond to the average of $d_P$ and $d_D$, respectively. For instance, for **13**, there is a large density of occurrence of short distances in $d_P$ (marked with the letter P) and long distances in $d_D$. Those conformations would allow for ready oxidative addition of C–$Br_P$, consistent with the experimental observation of oxetane formation. Notice that high density of distances also occurs in the upper right quadrant (marked as X). However, these points correspond to non-reactive conformations as both $d_P$ and $d_D$ are clearly too large. A similar map can be observed for **19**, except that now there are noticeable patches of short $d_D$ distances and long $d_P$ distances (marked as D). Remarkably, this is consistent with the observed 1 : 1 ratio in the outcome of the reaction. For **2a**, the highest density of reactive conformations occurs for short $d_D$ distances and relatively long $d_P$ distances. As a consequence, C–$Br_P$ becomes, on average, less accessible to the Cu-complex, and oxidative addition involving C–$Br_D$ becomes more probable, consistent with the formation of dihydrofuran **3a**. Areas with too short distances are also non-reactive. The distribution of distances for **7** and **2k** are similar to **2a** in that the larger occurrence corresponds to C–$Br_D$ selectivity, also consistent with major formation of dihydrofuran. Interestingly, the maps for **7** and **2k** are similar to each other in that the proportion of non-reactive conformations (X) is larger than the reactive conformations. This is consistent with the low conversions we observed for each of these in acetonitrile at 80 °C.

Using MD simulations on just the substrates is attractive in its simplicity. In these cases, where electronic effects can be ruled out and where the two products are likely to result from the same basic pathways, the outcome of the molecular mechanics simulations provides a useful framework for thinking about altering the product distributions.

While the simulations did not include anything related to the catalyst system, it is clear that Cu, its counterion, and the ligand could all influence conformation populations of $d_P$ and $d_D$. Although it is not completely straightforward to predict how changes in the catalyst system will affect the balance of products, the understanding that conformation populations play a critical role gave us a clue. For example, **2a** under the conditions of procedure A gives solely **3a**. The result was the same using CuBr, rather than CuI (procedure C). However, in the absence of a ligand (all other conditions same as procedure C), CuBr provided **3a** : **4a** in a 70 : 30 ratio. The reaction was slower (3 d), but conversion to the two products was clean. Clearly, the presence or absence of a ligand would impact conformational populations. While the MD simulations with just the starting alcohols did not in themselves reveal how altering the catalyst/ligand would shift the outcome, they did importantly reveal factors to explore.

To illustrate the utility of the 4-bromodihydrofuran products, **3a** was coupled with phenyl boronic acid and **3b** with phenyl acetylene under standard conditions for the Suzuki–Miyaura and Sonogashira reactions, respectively. Coupled products **22** (61%) and **23** (74%) were isolated in good yields. We also prepared 4-bromodihydrofuran **3o**, an intermediate from the patent literature used to prepare pesticides *via* subsequent coupling reactions (Scheme 3).[23] Our three step process from commercial ketone provided **3o** in 31% overall yield. The catalysts and ligand used in the sequence are inexpensive and relatively innocuous. The five step route to such trifluoromethylaryl ketone derived 4-bromo-2,3-dihydrofurans reported in the patent literature used a relatively expensive Rh catalyst and ligand and required the use of an autoclave, $Br_2$ and CO. The straightforward preparation of **3o** illustrates the utility of this three step preparation of 4-bromodihydrofurans.

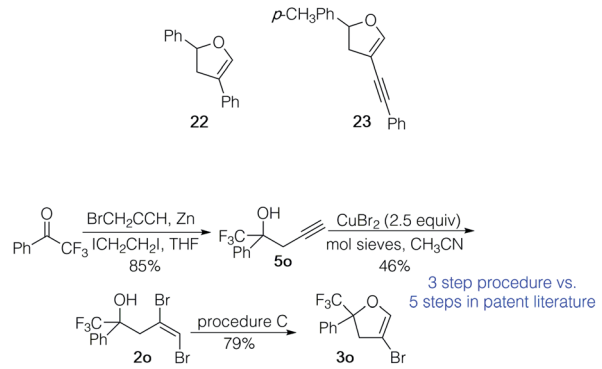


Scheme 3 Preparation of patented pesticide precursor **3o**.

## Conclusions

In conclusion, we have developed a straightforward, efficient three step approach to 4-bromo-2,3-dihydrofurans from aldehydes and ketones. These dihydrofurans are usefully functionalized for subsequent coupling reactions and potential reduction of the alkene to provide tetrahydrofurans. The key transformation involved the possibility of a 4-*exo* or 5-*endo* Cu(I) catalyzed *O*-vinylation of a dibromoalkene in which the latter cyclization predominated. On the other hand, direct competition with divinylalcohol **19**, containing appropriately positioned vinylbromide moieties, demonstrated that the 4-*exo* and 5-*endo* modes were essentially equally likely to occur. An electronic explanation for the preference for 5-*endo* products was ruled out *via* a combination of force field conformational search and DFT. On the other hand, MD simulations, using just the alcohols and based on two key geometric parameters, $d_P$ and $d_D$, provided a qualitative rationalization for product distributions between oxetane and dihydrofuran with key representative compounds. These experimental and computational studies have provided important clues for understanding and influencing these useful Ullmann-type cyclizations.

## Author contributions

J. A., J. I. and T. K. contributed to the experimental work; J. A. G. and A. R. contributed to the computational work. J. A., J. A. G. and A. R. H. contributed to ideation and writing of the paper.

## Conflicts of interest

There are no conflicts to declare.

## References

1 J. Cornil, L. Gonnard, C. Bensoussan, A. Serra-Muns, C. Gnamm, C. Commandeur, M. Commandeur, S. Reymond, A. Guérinot and J. Cossy, *Acc. Chem. Res.*, 2015, **48**, 761–773.
2 Q. Lu, D. S. Harmalkar, Y. Choi and K. Lee, *Molecules*, 2019, **24**, 3778pp.
3 A. S. Dudnik and V. Gevorgyan, *Angew. Chem., Int. Ed.*, 2010, **49**, 2096–2098.
4 P. Ruiz-Castillo and S. L. Buchwald, *Chem. Rev.*, 2016, **116**, 12564–12649.
5 M. K. Lakshman and P. K. Vuram, *Chem. Sci.*, 2017, **8**, 5845–5888.
6 K. Morimoto, *Chem. Pharm. Bull.*, 2019, **67**, 1259–1270.
7 I. Kanwal, A. Mujahid, N. Rasool, K. Rizwan, A. Malik, G. Ahmad, S. A. Shah, U. Rashid and N. M. Nasir, *Catalysts*, 2020, **10**, DOI: 10.3390/catal10040443.
8 A. Taheri Kal Koshvandi, M. M. Heravi and T. Momeni, *Appl. Organomet. Chem.*, 2018, **32**, e4210.
9 C. A. Malapit, I. K. Luvaga, D. R. Caldwell, N. K. Schipper and A. R. Howell, *Org. Lett.*, 2017, **19**, 4460–4463.
10 K. Camara, S. S. Kamat, C. C. Lasota, B. F. Cravatt and A. R. Howell, *Bioorg. Med. Chem. Lett.*, 2015, **25**, 317–321.
11 R. Raju and A. R. Howell, *Org. Lett.*, 2006, **8**, 2139–2141.
12 Y. Fang and C. Li, *J. Am. Chem. Soc.*, 2007, **129**, 8092–8093.
13 S. Bhunia, G. G. Pawar, S. V. Kumar, Y. Jiang and D. Ma, *Angew. Chem., Int. Ed.*, 2017, **56**, 16136–16179.
14 C. Sambiagio, S. R. Marsden, A. J. Blacker and P. C. McGowan, *Chem. Soc. Rev.*, 2014, **43**, 3525–3550.
15 G. Chelucci, *Chem. Rev.*, 2012, **112**, 1344–1462.
16 A. S. Y. Lee, S. F. Chu, Y. T. Chang and S. H. Wang, *Tetrahedron Lett.*, 2004, **45**, 1551–1553.
17 J. Xiang, R. Yuan, R. Wang, N. Yi, L. Lu, H. Zou and W. He, *J. Org. Chem.*, 2014, **79**, 11378–11382.
18 L. M. Dollinger and A. R. Howell, *J. Org. Chem.*, 1996, **61**, 7248–7249.
19 G. O. Jones, P. Liu, K. N. Houk and S. L. Buchwald, *J. Am. Chem. Soc.*, 2010, **132**, 6205–6213.
20 H.-Z. Yu, Y.-Y. Jiang, Y. Fu and L. Liu, *J. Am. Chem. Soc.*, 2010, **132**, 18078–18091.
21 K. Roos, C. Wu, W. Damm, M. Reboul, J. M. Stevenson, C. Lu, M. K. Dahlgren, S. Mondal, W. Chen, L. Wang, R. Abel, R. A. Friesner and E. D. Harder, *J. Chem. Theory Comput.*, 2019, **15**, 1863–1874.
22 A. D. Bochevarov, E. Harder, T. F. Hughes, J. R. Greenwood, D. A. Braden, D. M. Philipp, D. Rinaldo, M. D. Halls, J. Zhang and R. A. Friesner, *Int. J. Quantum Chem.*, 2013, **113**, 2110–2142.
23 P. Bindschädler, G. K. Datta and W. Von Deyn, *World Pat.*, WO2016102490A1, 2016.